

# NON-ISOTHERMAL, NON-NEWTONIAN ANALYSIS OF THREE DIMENSIONAL RTM/VARTM PROCESSES USING HP-ADAPTIVE FINITE ELEMENT METHOD

Ravi Mayavaram, Mahender Reddy,  
The Computational Mechanics Company, Inc.

7800 Shoal Creek Blvd, Suite 290E, Austin, TX 78757.

David Stewart, and John Tolle  
Stewart Automotive Research, LLC

1260 Shotwell Dr., Houston, TX 77020.

## Abstract

A numerical analysis of the RTM/VARTM processes using an *hp*-adaptive finite element method is presented in this paper. The constitutive behavior of the resin is modeled using the Carreau-Yasuda 5-parameter model with the WLF and the Arrhenius functions for describing the temperature dependence of the viscosity. In addition, the viscosity can also be read in as a tabular function of the effective shear rate and the temperature. The RTM process is modeled as a three-dimensional, two-phase flow of resin and air (weakly compressible fluid) using a modified Darcy's model. Examples demonstrating the role of SUPG smoothing, viscosity variation, vacuum conditions, and dynamic adaptivity are presented in this work.

## 1. Introduction

### 1.1 Process Description

Resin transfer molding and its variants are used to manufacture polymeric composites. A general introduction on this subject is available in references 1 and 2. In the present form these methods do not meet the requirements for the mass production of polymeric composites. The industry, however, is attempting devise techniques to achieve this goal as we prepare ourselves for the next century. In this context, numerical simulation of RTM and its variants can help to design, predict, and analyze the complex dynamics of the filling process.

### 1.2 Brief Background

A brief review of available literature in the field of numerical studies related to RTM is presented here. We have summarized the different aspects of RTM simulation in the context of isothermal and non-isothermal analyses in our previous work [3,4]. Unfortunately, very little published literature is available on non-Newtonian flow simulations of RTM. Lin and Hahn [5] present an analysis using a power-law model and their viscosity depends on  $(|\mathbf{v}|/H)$  instead of the shear rate, and  $H$  is the depth of the mold. This definition will not be very useful in complete 3D analysis and one should use the second invariant of the rate of deformation tensor as a measure of the shear rate. Their work uses the Arrhenius function for temperature dependence. Besides the Arrhenius function, another approach is to use the WLF (William-Landel-Ferry) function [6]. Sometimes a simplified form of Arrhenius

function such as  $\exp(-b(T-T_0))$  is used [7], but such approximations are valid only over a very small range of temperature and useful for analytical calculations.

One of the major deficiencies of a power-law fluid is the lack of a zero shear limit and hence, its predictions become worse as the shear rate tends to zero [6]. The 5-parameter Carreau-Yasuda model overcomes this deficiency by having well-posed limits for both zero shear and the infinite shear viscosity. Analysis of non-Newtonian flow in context of pore-level flow is discussed under many sections in Advani [2]; however, there is a dearth of published literature for overall numerical analysis of RTM using non-linear fluid models for resin.

### 1.3 Present Work

This work is a continuation of our numerical studies presented in references 3 and 4. In this paper, the role of SUPG (Stream-wise Upwind Petrov Galerkin) smoothing in solving advection dominated problems, temperature dependence of viscosity, nonlinear nature of viscosity, the role of dynamic adaptivity, and the effect of vacuum pressure in VARTM processes are discussed. These issues are important in achieving an accurate simulation of the RTM processes.

## 2. Proposed Method

The infusion of resin in a porous preform is modeled as a transient, three dimensional, nonisothermal, non-Newtonian, weakly compressible, two-phase flow of a resin and air in a porous media. This model accurately describes the physics of the process. In this section we describe the governing equations, the boundary conditions, and the numerical method.

### 2.1 Governing Equations

#### Conservation of Mass:

The mass conservation equation for the resin and air are given in equation (1). The suffixes 1, 2, and 3, indicate properties of the resin, air, and the preform, respectively. The flow domain  $\Omega \subset \mathbf{R}^3$  is three dimensional and its boundary is denoted by  $\Gamma \subset \mathbf{R}^2$ .

$$\partial(\phi S_i)/\partial t = -\nabla \cdot (\rho_i \mathbf{v}_i) \quad i = 1, 2 \quad \text{in } \Omega \quad (1)$$

Where  $\phi$  denotes the porosity,  $\rho_i$ ,  $S_i$ , and  $\mathbf{v}_i$  are the density of the fluid, the phase saturation, and the phase velocity vector, respectively. Since,  $S_1 + S_2 = 1$ , it suffices to compute the saturation of resin.

**Conservation of Momentum:**

Darcy's law describes the momentum dynamics in a porous media completely saturated with a fluid. In the case of a two phase flow model, Darcy's law is modified using the relative permeability function [3] to account for the presence of two fluids. The modified Darcy's model is given by  $\mathbf{v}_i = \mathbf{m}_i \nabla p_i - \rho_i \mathbf{g} \nabla D$ , where  $D$  denotes the depth and  $\mathbf{m}_i$  denotes the mobility of the phase  $i$  and it is given by the expression  $(\mathbf{m}_i = \mathbf{k} k_{ri} / \mu_i)$ . Here,  $\mathbf{k}$  is the absolute permeability tensor for the fiber preform,  $k_{ri}$  is the relative permeability of the phase  $i$ , and  $\mu_i$  is the dynamic viscosity of phase  $i$ .

**Model equations for average Pressure and Saturation:**

The above equations can be rearranged into a parabolic equation describing the average pressure and an hyperbolic equation describing the saturation of the resin. The average pressure,  $P$  is the average of the phase pressures which is given by,  $P = (P_1 + P_2) / 2$  and the capillary pressure,  $P_c$  is given by the difference,  $P_c = P_2 - P_1$ . To close the system of equations, the capillary pressure is empirically specified.

$$\phi C_1 (\partial P / \partial t) = \tilde{N} \cdot ((\mathbf{m}_1 + \mathbf{m}_2) \cdot \tilde{N} P) + \frac{1}{2} \tilde{N} \cdot ((\mathbf{m}_2 - \mathbf{m}_1) \cdot \tilde{N} P) - g \tilde{N} \cdot ((\mathbf{m}_1 \rho_1 + \mathbf{m}_2 \rho_2) \cdot \tilde{N} D) \quad (2)$$

$$\mathbf{v}_t = \mathbf{v}_1 + \mathbf{v}_2 \quad (3)$$

$$\phi (\partial S_1 / \partial t) = \tilde{N} \cdot (\mathbf{h}_1 \cdot \tilde{N} S_1) - \tilde{N} \cdot (f_1 \mathbf{v}_t) - \tilde{N} \cdot (\mathbf{G}_1 \cdot \tilde{N} D) \quad (4)$$

where  $\mathbf{v}_t$  is the total velocity vector, the fractional flow coefficient  $f_1 = \mathbf{m}_1 / (\mathbf{m}_1 + \mathbf{m}_2)$ , the capillary term  $\mathbf{h}_1 = -\mathbf{m}_2 f_1 (d p_c / d S_1)$  and the gravity term  $\mathbf{G}_1 = f_1 (\rho_1 + \rho_g) \mathbf{g} \mathbf{m}_2$ . The total compressibility,  $C_1$  is the sum of the individual compressibilities of the resin, air, and the preform.

**Conservation of Energy:**

A local equilibrium temperature  $T$  is defined and the heat transfer in the domain is studied using a single energy equation. The thermal conductivity is assumed be in parallel between the preform and the fluids, and in sequential mode between the fluids. Hence the equivalent thermal conductivity  $\kappa$  is given by the expression  $\kappa = (1 - \phi) k_3 + \phi k_1 k_2 / (k_1 S_1 + k_2 S_2)$ . Equation (5) describes the energy equation. The terms  $\alpha$  and  $\beta$  denote the averaged capacitance coefficients and are given by  $\alpha = (\rho C_p)_1 S_1 + (\rho C_p)_2 S_2$  and  $\beta = (\rho C_p)_3 (1 - \phi) + \alpha$ , respectively.

$$\beta (\partial T / \partial t) + \alpha \mathbf{v}_t \cdot \tilde{N} T = \tilde{N} \cdot (\mathbf{k} \cdot \tilde{N} T) \quad (5)$$

**2.2 Material Non-linearity**

**Carreau-Yasuda Model:**

The constitutive behavior of the resin is described using this 5-parameter model. This model defines two

limiting viscosities: zero shear viscosity and infinite shear viscosity. The following equation defines the Carreau-Yasuda model.

$$\mathbf{h} = \mathbf{h}_\infty + (\mathbf{h}_0 - \mathbf{h}_\infty) \left[ A + (\mathbf{I} \dot{\mathbf{g}})^a \right]^{\frac{n-1}{a}} \quad (6)$$

By choosing the appropriate values for the different parameters, a wide variety of generalized Newtonian models can be obtained. The above model actually has six additional parameters, the additional parameter being  $A$ , which is the "Zero Shear Constant". The original model uses the value 1 instead of this parameter. The other parameters are: the time constant ( $\lambda$ ), the transition parameter  $a$ , the zero shear viscosity  $\eta_0$ , the infinite shear viscosity  $\eta_\infty$ , and the power law index  $n$ . The effective shear rate  $\gamma$  is defined as the second invariant of rate of deformation tensor. The viscosity computed depends on the temperature. Two different temperature functions are used in the work and they are the Arrhenius and the WLF (Williams-Landel-Ferry) functions.

$$\mathbf{h}(T) = \mathbf{h}(T_g) \exp \left[ \frac{-C_1^g (T - T_g)}{C_2^g + (T - T_g)} \right] \quad (7)$$

The above equation represents the WLF transformation with two constants  $C_1$  and  $C_2$  with glass transition temperature (superscript  $g$ ) as the reference. The other function used is the Arrhenius transformation which involves a single parameter, "Activation Energy".

$$\mathbf{h}(T) = \mathbf{h}(T_0) \exp \left[ \frac{\Delta E}{RT} \right] \quad (8)$$

The viscosity distribution can be specified as a data table of two independent variables, the shear rate and the resin temperature. Often, raw data is available such formats and enabling the analysis to use the raw directly rather than a fitted model is more accurate.

**2.3 Boundary and Initial Conditions**

The boundary of the domain consists of the inlet gates, the exit vents, the solid walls of the mold, and the symmetry planes. For the pressure equation, either the pressure or the fluxes should be specified on all boundaries, as this equation is elliptic in space and parabolic in time. The saturation equation is hyperbolic, hence it is only necessary to specify the value of saturation of resin (which is 1) at the inlet boundaries. The velocities are post computed using the pressure distribution. An accurate specification of boundary conditions for the pressure equation is sufficient for the velocity equations. The energy equation is also parabolic in time and elliptic in space, hence, either temperature or the heat flux must be specified on all boundaries. Initial conditions for the

pressure, saturation, and the temperature should be specified through out the domain  $\Omega$ .

## 2.4 Finite Element Model

The code based on the above model equations is built using the powerful *hp*-adaptive library ProPHLEX [8]. This code (**PHLEXrtm**) has the capability for both manual adaptivity, and automatic adaptivity based on error estimates. The latter option includes dynamic adaptivity as well. The elements in the mesh can be refined (or unrefined) and enriched (or un-enriched). This makes it possible to use an optimal mesh even to capture front movements.

## 3. Results and Discussion

### 3.1 SUPG Smoothing

The effect of SUPG smoothing is demonstrated using the infusion of a beam shown in the figure 1. The governing equation for resin saturation is hyperbolic. The traditional finite element method loses its "*best approximation property*" for such equations and it is under-diffusive. This is often overcome by using methods like SUPG smoothing, however, these methods sometimes result in being over-diffusive and smear the resin saturation front. These techniques are also required for the energy equation as the heat transfer is advection dominated in the filling process. Figures 2 and 3 show how these methods can be controlled using a smoothing factor that takes a value between 0 and 2. The value to be selected is not constant and depends on the problem data. Further research is necessary to optimize the selection of this parameter based on the problem data.

### 3.2 Viscosity vs. Temperature

The resin viscosity is a strong function of temperature. Figure 4 shows how the resin viscosity changes with temperature in a filling process for Arrhenius function and WLF function. The values for parameters in these functions are chosen from references 5 and 6. It should be noted that the equations are strongly coupled and any change in viscosity affects the prediction of the pressure and which in turn affects the saturation, velocity and temperature.

### 3.3 VARTM: The effect of Vacuum Pressure

The effect of vacuum pressure is demonstrated using the table 1. This clearly indicates the need for modeling both the resin and air phases. The vacuum pressure in the order of 1000 Pa (absolute,  $\sim 5$  Torr) is required to ensure complete filling, otherwise the residual air trapped inside the mold would inhibit the process. Since the injection is pressure driven, depending on the compressibility of the air, which depends on the vacuum pressure, the pressure in the mold will attain equilibrium before part is completely filled.

## 3.4 Dynamic Adaptivity

The resin infusion and other filling problems require dynamic adaptivity to track the movement of the resin front. Figure 5 shows the viscosity distribution used for the resin for this problem. An initial mesh with 100 elements is shown in the figure 6. Figures 7 and 8 shows the adapted mesh at two different time steps. The mesh adaptation following the resin front is clearly seen in the figures. This refinement and unrefinement strategy leads to optimal mesh density without compromising on accuracy. The temperature distribution and the resin saturation in the domain (for the mesh in figure 8) are shown in figures 9 and 10. The mesh adaptation is based on the resin saturation distribution, however, research is underway for computing the error-estimate based on both the resin saturation and temperature distribution.

## 4. Conclusions

The results shown demonstrate some of the advanced model features of PHLEXrtm and its potential use in industry. More results with experimental validation (tests conducted at the test facility of Stewart Automotive Research) will be presented at the conference.

## Acknowledgements

This work has been supported in part by National Institute of Standards and Technology's Advanced Technology Program.

## References

1. Potter, K., *An Introduction to Composite Products*, Chapman & Hall, London, 1997.
2. Advani, S. G (Ed.), *Flow and rheology in polymer composite manufacturing*, Elsevier, Amsterdam, (1994).
3. Deb, M., Reddy, M., Mayavaram, R., and Baumann, C., Paper #467, presented in ANTEC 1998, Atlanta, GA, (1998).
4. Mayavaram, R., Reddy, M., and Stewart, David, Paper #743, Presented in ANTEC 1999, New York, NY (1999).
5. Lin, M. Y., and Hahn, H. T., XII Technical Conference of American Society for Composites, Dearborn, MI, (1997).
6. Bird, R. B., *et al.*, "*Dynamics of Polymeric Liquids: Vol. 1*", Wiley, New York, NY (1987).
7. Brusckhe, M. V. and Advani, S. G, *Journal of Rheology*, **37**, pp. 479-498, (1993).
8. ProPHLEX: An *hp*-Adaptive Finite Element Kernel, Computational Mechanics Company (1996).

## Keywords

Resin transfer molding, finite elements, non-isothermal, non-Newtonian

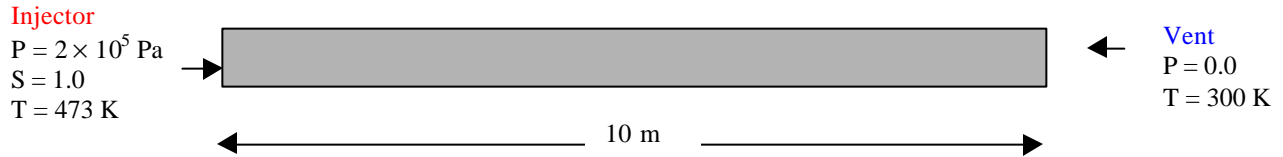


Figure 1. Resin infusion in a beam. One-dimensional filling example for demonstrating the model features.

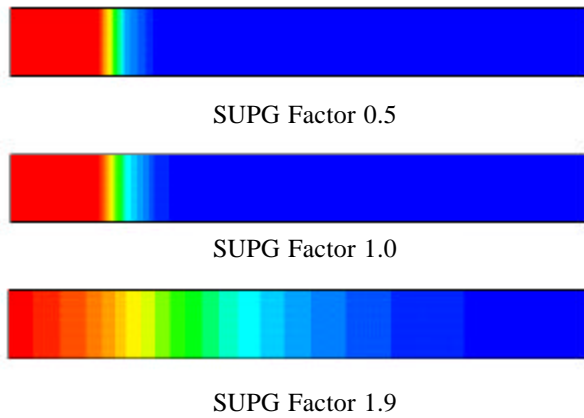


Figure 2. Smearing of the saturation front for different SUPG factors.

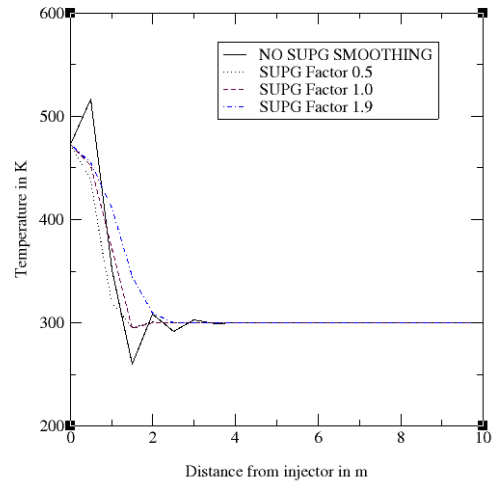


Figure 3. SUPG smoothing for advection dominated heat transfer during resin infusion.

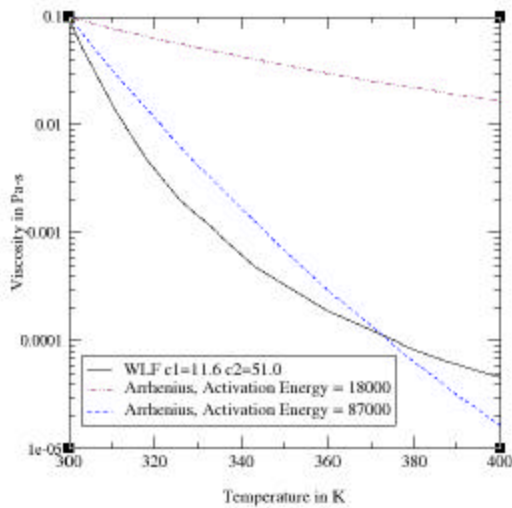


Figure 4. Variation of the resin viscosity with temperature for WLF and Arrhenius transformations.

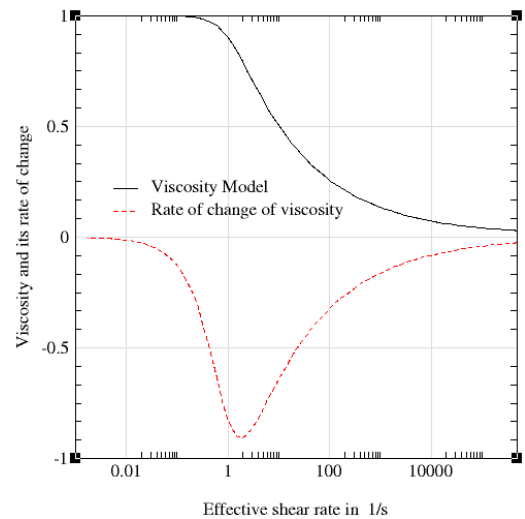


Figure 5. Viscosity and its rate of change as function of effective shear-rate.

Air Density	Vacuum Pressure	Fill %
1.0	1.0E+05	30
0.12	1.0E+04	84
0.02	1.0E+03	100

Table 1: Fill % as a function of vacuum pressure

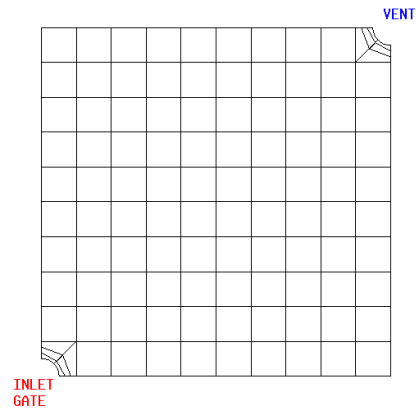


Figure 6. Initial mesh used for the analysis

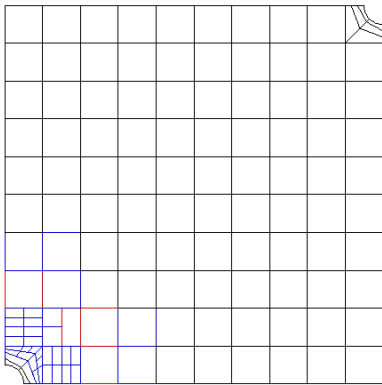


Figure 7. Adapted mesh after few time steps. Blue color indicates quadratic and red indicates cubic edges.

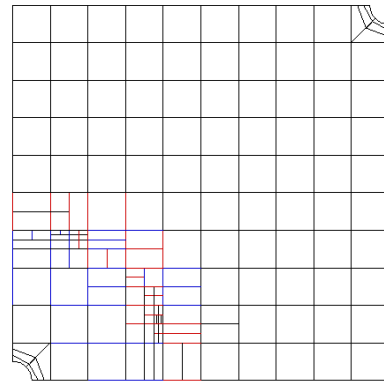


Figure 8. Adapted mesh after the front has progressed further. Blue color indicates quadratic and red indicates cubic edges.

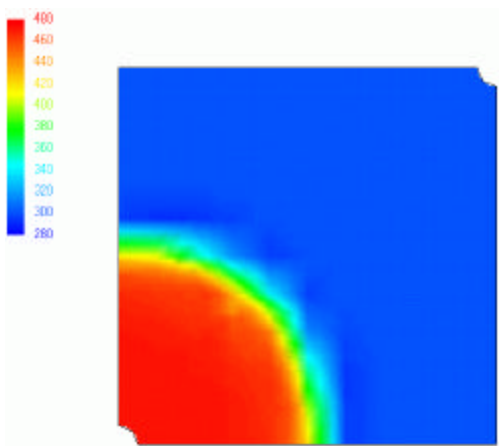


Figure 9. Temperature distribution in the domain for the mesh shown in the figure 8.

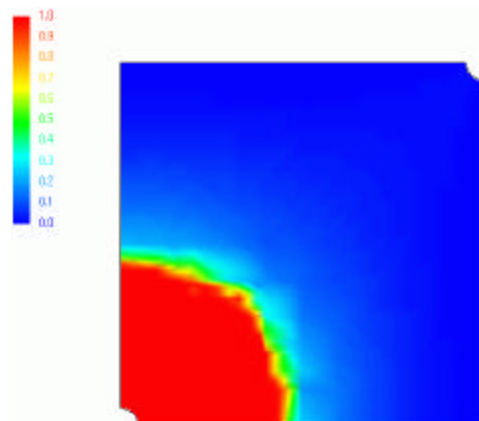


Figure 10. Resin saturation in the domain for the mesh shown in the figure 8.